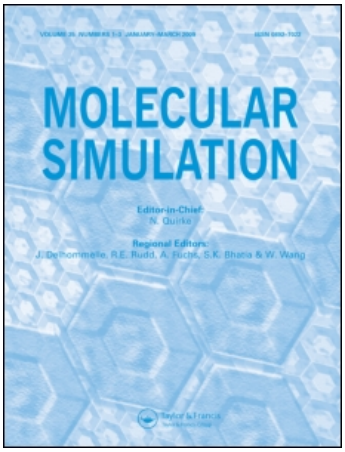

Molecular Simulation
Publication details, including instructions for authors and subscription information:
http://www.informaworld.com/smpp/title~content=t713644482

Atomistic Simulation of Mineral Surfaces

N. H. De Leeuw[a]; S. C. Parker[a]
[a] School of Chemistry, University of Bath, UK

To cite this Article De Leeuw, N. H. and Parker, S. C.(2000) 'Atomistic Simulation of Mineral Surfaces', Molecular Simulation, 24: 1, 71 — 86
To link to this Article: DOI: 10.1080/08927020008024188
URL: http://dx.doi.org/10.1080/08927020008024188

Molecular Simulation, 2000, Vol. 24, pp. 71–86
Reprints available directly from the publisher
Photocopying permitted by license only

ATOMISTIC SIMULATION OF MINERAL SURFACES

N. H. DE LEEUW and S. C. PARKER*

School of Chemistry, University of Bath, Claverton Down, Bath Ba7 2AY, UK

(Received June 1999; accepted June 1999)

Atomistic simulation techniques are now able to model the structure of mineral surfaces at the atomic level. In this paper we begin to address the question of whether surface reactivity can be studied reliably by modelling the surface reactivity of calcite, fluorite and forsterite under aqueous conditions. We first used energy minimisation techniques to investigate the interaction between the minerals calcite and fluorite with water and methanoic acid. The relative adsorption energies suggest that methanoic acid preferentially adsorbs onto fluorite surfaces, while water adsorbs preferentially onto calcite as inferred from experiments on mineral separation. Molecular Dynamics simulations were also used to model the effect of temperature on the adsorption of water on the calcite $\{10\bar{1}4\}$ and fluorite $\{111\}$ surfaces. Furthermore we used these techniques to model point defect formation at surfaces. We are also interested in modelling the competition between associative and dissociative adsorption on mineral surfaces. Simulations of adsorption of water on the low-index forsterite surfaces have predicted the adsorption energies and equilibrium morphology. The calculated equilibrium morphology adequately reproduces the experimental morphology of forsterite suggesting that the relative stabilities of the surfaces, both unhydrated and hydroxylated, are calculated correctly.

Keywords: Mineral surfaces; low-index; fluorite surfaces; cleavage planes; energy minimization

INTRODUCTION

The aim of our work is to model the surface structure and reactivity of minerals at the atomic level. In this paper we describe our progress on a number of minerals, namely calcium carbonate, calcium fluoride and forsterite, and for reactivity we have chosen to model their interaction with water. In earlier work [1–5] we have shown that simulation techniques can model the interaction of water with perfect surfaces. We are now

*Corresponding author. e-mail: s.c.parker@bath.ac.uk

attempting to extend this in two ways by, first, studying the energetics of competitive adsorption such as illustrated by the competitive adsorption of water and methanoic acid which is of relevance to mineral separation techniques and, secondly, modelling the interaction of an adsorbate with surface defects, that are likely to be present on real crystals. At present atomistic simulation techniques represent the best way of rapidly modelling many different surfaces of different materials. The basis of this approach is the Born model of solids where simple parameterised analytical equations are used to describe the forces between atoms. Although a full electronic structure calculation is preferred the inherent speed of atomistic simulations allows us to examine many different models of different surfaces with a high level of complexity which can be used as an aid to the interpretation of experiment and thus provide a useful complement to experimental structural techniques, provided of course that the methods are reliable. There are now many examples in the literature where there is good agreement between the structural models developed by the atomistic simulation methods and those observed by experiment. Such examples include the surfaces of rutile [6], alumina [7] and tungsten oxide [8]. In addition to giving good structural information these techniques also provide detailed energetics and where there are available experimental data the energies of adsorption of water, for example on magnesia, calcia [9] and alumina [5, 10] are in good agreement. The level of agreement between simulation and experiment gives us sufficient confidence to apply these techniques to problems where there are much less experimental data. Two such areas which we have started to investigate are the processes involved in the separation of different minerals from aqueous solution, and crystal growth as exemplified by calcite. However, before discussing these applications we still briefly review the methods.

THEORETICAL METHODS

The atomistic simulation of the surfaces of polar solids was pioneered by the work of Tasker [11, 12] and Mackrodt and Stewart [13]. The low energy, and hence the most common, surfaces of a crystal are generally those of low Miller index. These planes are the closest packed and hence have the smallest surface area per unit cell. As the unit cell volume is fixed these will have the largest interplanar spacings, they will then be most easily cleaved and hence have the lowest surface energy. However in polar solids other factors apply, for example the electrostatic contribution. Bertaut

[14] demonstrated that when there is a dipole moment perpendicular to the surface, the surface energy diverges and increases with increasing size. The surface must therefore be constructed with no net dipole perpendicular to the surface [11]. Thus surfaces which are made of alternating charged planes, called dipolar (or polar) surfaces cannot occur naturally without the adsorption of foreign atoms or surface roughening [15]. As a way of identifying these potentially unstable surfaces Tasker [12] characterized the surfaces in terms of the repeat unit which when repeated into the bulk generates the crystal. He identified three types of surface, type I in which the repeat unit is charge neutral stoichiometric layers, type II which is comprised of charged layers but in such a way that there is no dipole moment perpendicular to the surface and finally type III where there is such a dipole moment, which has to be modified in some way to remove the dipole.

There are two strategies for generating a simulation cell for modelling free surfaces. One is to use a two region approach and 2-dimensional periodicity is assumed. The crystal is divided into two regions; a region I adjacent to the interface where the ions are allowed to move independently and a region II in which the ions are held fixed relative to each other but the region as a whole may move. The inclusion of a region II ensures that all the energies of the ions in region I are fully converged. The second approach is to take only region I and assume three-dimensional periodicity. Thus the simulation cell comprises a slab of solid separated by a vacuum gap or fluid which is then repeated infinitely. The virtue of this approach is that it is possible to exploit the periodicity to ensure that the energies, particularly the electrostatic component, of large simulation cells can be calculated rapidly using efficient algorithms but the disadvantage is that as a consequence of the long range nature of the electrostatic forces the ions on one surface may be influenced by the behaviour of ions on the other.

Once the energies and forces are evaluated we next apply either energy minimisation or molecular dynamics simulation techniques. Energy minimisation is achieved by adjusting the atoms in region I until the net forces on each atom are zero. Molecular dynamics allows explicit treatment of temperature by giving all the ions in region I kinetic energy. Generally, we begin by using energy minimisation to evaluate the surface structure and energy of a range of surfaces and select suitable candidate surfaces for further study with molecular dynamics. Again we first investigate the surface structure and energy before considering dynamical properties, such as molecular transport. The simulations are all performed assuming constant area.

The potential parameters used for the simulation of the calcite crystal are those derived by Pavese *et al.* [16] in their study of the thermal dependence of structural and elastic properties of calcite while the potential model used for fluorite was derived by Catlow *et al.* [17]. The potential parameters for forsterite were those derived for MgO by Lewis and Catlow [18] and SiO_2 by Sanders *et al.* [19], used successfully in earlier simulations of bulk properties of forsterite, *e.g.*, Price *et al.* [20] and Parker and Price [21]. The inter- and intramolecular interactions of the water molecules were derived by ourselves [3]. The calcite/water interactions were verified against the structure of the calcium carbonate hexahydrate ikaite as described previously [4], and the close agreement between experimental and calculated structure and formation energies means that we may be confident that the potential parameters describe the water/surface interactions adequately. The methanoic acid molecule was modelled using the cvff forcefield [22]. The interactions between the minerals and the methanoic acid molecules were again adapted according to the charges on the atoms.

Competitive Adsorption of Water and Methanoic Acid onto Calcite and Fluorite Surfaces

Calcite has a rhombohedral crystal structure not unlike distorted rock salt [23]. The $\{10\bar{1}4\}$ cleavage plane is by far the most stable surface of calcite and dominates the morphology, usually to the exclusion of other surfaces both in ultra-high vacuum conditions [24, 25] and in aqueous environment [26–28]. We may therefore expect the calcite crystals in the mineral mixture to express the $\{10\bar{1}4\}$ surface and as such we have concentrated on this surface. The $\{10\bar{1}4\}$ surface is a type I surface consisting of layers of both calcium atoms and carbonate groups. Both calcium atoms and oxygen atoms are easily accessible to adsorbing molecules from solution. Fluorite has a cubic crystal structure. The most stable surface is the $\{111\}$ cleavage plane, which is a type II surface consisting of planes of calcium ions in a hexagonal array with a layer of fluorine ions both above and below. The surface is thus terminated with fluorine atoms although the calcium ions are still accessible to adsorbing molecules.

Associative adsorption of water molecules onto the calcite plane stabilises the surface, lowering the surface energy [4, 28]. The surface energy of the hydrated surface ($\gamma = 0.17\,Jm^{-2}$) is in good agreement with the surface energy found experimentally for the cleavage plane of calcite of $0.23\,Jm^{-2}$ [29], particularly when taking into account that the experimental surface was mechanically cut and will contain steps and other dislocations

which will increase the surface energy. The lattice spacing (Ca – Ca = 4.0 and 4.8 Å) is large enough for a water molecule to adsorb by its oxygen atom to each calcium atom in a herringbone pattern (Fig. 1). In addition, the calculated hydration energy of $-92.2\,\mathrm{kJmol^{-1}}$ is in good agreement with the binding energy of $-110.9\,\mathrm{kJmol^{-1}}$ quoted by Liang *et al.* [30] for water molecules adsorbed onto calcite.

The fluorite {111} surface is also stabilised by the associative adsorption of water and remains the dominant surface. Unlike calce, the hexagonal pattern of surface calcium atoms (and fluorine atoms) with interatomic spacing of 3.85 Å is too small for one water molecule to adsorb on each calcium atom and instead only 50% of the available cation sites is covered by water molecules (Fig. 2).

We next considered adsorption of methanoic acid molecules to the surfaces. The lattice spacing on the calcite surface, which was large enough to allow full monolayer coverage of water molecules, is not large enough to accommodate one HCOOH molecule per surface calcium atom. Instead, only one methanoic acid molecule is adsorbed for each two surface calcium atoms in a regular pattern. On the fluorite {111} surface the methanoic acid molecules adsorb more strongly than onto calcite. As noted above the interatomic distance is even smaller than for calcite and, as with water, only a fifty percent coverage can be accommodated. This coverage is reasonable if we compare with experimental work by Mielczarski *et al.* [31]

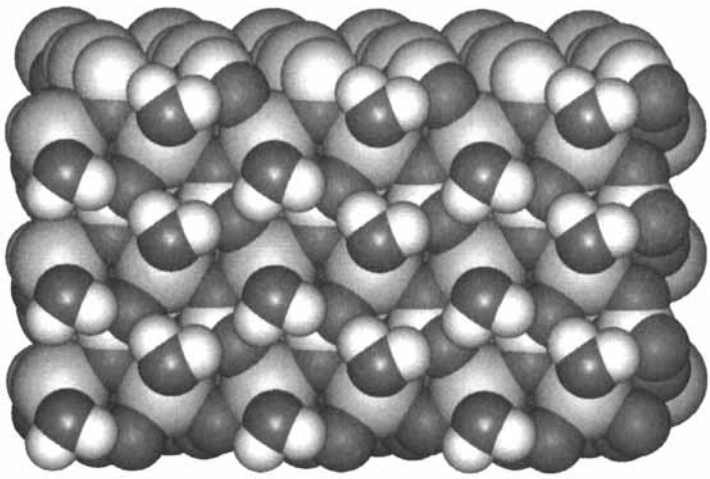

FIGURE 1 Plan view of the calcite surface with adsorbed water molecules (Ca = green, C = yellow, O = red, O_{water} = blue, H = white). (See Color Plate I).

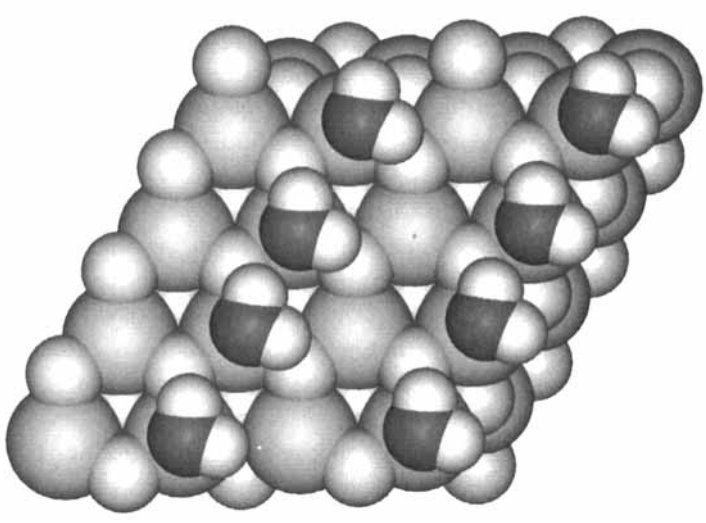

FIGURE 2 Plan view of the fluorite {111} surface with 50% partial coverage of water molecules (Ca = green, F = pale blue, O = red, H = white). (See Color Plate II).

who observed a 30% coverage of oleic acid molecules, which is a carboxylic acid with a long carbon chain rather than the hydrogen of methanoic acid. The methanoic acid molecules adsorb in a fairly flat configuration onto the surface, bridging between two calcium atoms by its oxygen atoms, and hydrogen-bonding by the hydroxyl hydrogen to two surface fluorine atoms (Fig. 3).

The adsorption energies for both water and methanoic acid onto both minerals are collected in Table II. The adsorption energies for methanoic acid onto the mineral surfaces are larger for fluorite than for calcite and as such methanoic acid would preferentially adsorb to fluorite over calcite when both minerals are present in a mixture. Furthermore, the adsorption energy for water on calcite is larger than for methanoic acid, probably due to both the very regular pattern of water adsorption with a network of hydrogen-bonding to surface oxygen atoms and to some steric effects of the larger acid molecules. Hence, the methanoic acid, which in mineral separation processes would be added to the minerals in the aqueous medium, would not be capable of displacing water from the calcite surface. In contrast, for the fluorite {111} surface, the adsorption energy for methanoic acid is considerably larger than for water due to the capability of the acid molecules to bridge by their oxygen atoms between two surface calcium atoms and the close hydrogen-bonding to surface fluorine atoms. Thus, on thermodynamic grounds it is energetically preferential for the

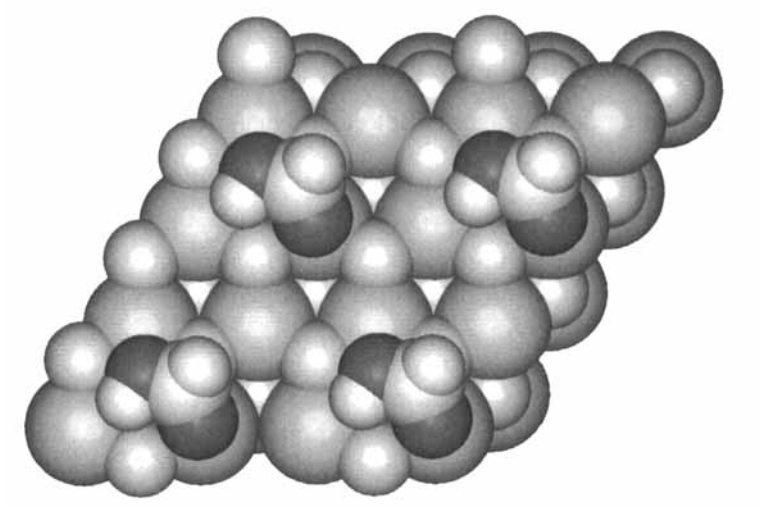

FIGURE 3 Plan view of the fluorite {111} surface with 25% partial coverage of methanoic molecules showing bridging of the methanoic acid molecules to two surface calcium atoms (Ca = green, F = pale blue, C = yellow, O = red, H = white). (See Color Plate III).

TABLE I Surface energies of pure and hydrated calcite and fluorite surfaces (Jm^{-2})

Mineral	*Surface*	*Unhydrated*	*Hydrated*
Calcite	$\{10\bar{1}4\}$	0.59	0.17
Fluorite	{111}	0.52	0.40

TABLE II Adsorption energies for water and methanoic acid onto calcite and fluorite surfaces ($kJmol^{-1}$)

Mineral	*Surface*	*Water*	*Methanoic acid*
Calcite	$\{10\bar{1}4\}$	−92.2	−84.2
Fluorite	{111}	−61.8	−102.4

methanoic acid molecules to adsorb to this surface displacing the water molecules from the adsorption sites.

Following the successful modelling of the mineral/water interface using static energy minimisation techniques, we were interested to study the effect of introducing temperature in our calculations and hence we used molecular dynamics simulations to investigate hydration of the calcite and fluorite cleavage planes.

Molecular Dynamics Simulation of Hydration of Calcite and Fluorite Cleavage Planes

In this section we describe recent molecular dynamics simulations, using the DL_POLY code [32], to investigate the interaction of water with the calcite $\{10\bar{1}4\}$ and fluorite $\{111\}$ cleavage planes at two temperatures, 300 K and 1000 K. However, 'real' surfaces are likely to contain a large number of defects. Therefore, we also consider the formation of a point defect on the surfaces and whether the structure and energies of adsorption are changed by introduction of a defect.

At 300 K, the water molecules adsorb onto the calcite $\{10\bar{1}4\}$ surface in the same regular herringbone pattern as observed using static energy minimisation techniques (Fig. 1). As expected, with the introduction of temperature the hydration energy has decreased to $-69.0\,\mathrm{kJmol^{-1}}$ (compared to $-92.2\,\mathrm{kJmol^{-1}}$ from the static calculations) (Tab. III). Once adsorbed the water molecules stay on the surface and do not diffuse through the gap. Figure 4 is a graph of the mean square deviation of the water molecules in the calcite and fluorite systems, clearly showing that on calcite the water molecules do not move with time. In contrast, the water molecules on the fluorite $\{111\}$ surface do not stay adsorbed on the surface but diffuse through the gap forming a droplet on the surface (Fig. 5). The diffusion coefficient of the water molecules is calculated to be $1.2 \times 10^{-9}\,\mathrm{m^2s^{-1}}$, which is identical to that calculated for water molecules in a box of pure liquid water at 300 K under NPT conditions [3]. The hydration energy is found to be $-47.4\,\mathrm{kJmol^{-1}}$ (compared to $-61.8\,\mathrm{kJmol^{-1}}$ from the static calculations) which is similar to the intermolecular interaction between water molecules themselves, calculated to be $-43.0\,\mathrm{kJmol^{-1}}$ in agreement with experiment ($-43.4\,\mathrm{kJmol^{-1}}$ [33]). Thus the water molecules do not bind strongly to the fluorite $\{111\}$ plane and

TABLE III Hydration energies of calcite and fluorite cleavage planes (300 K) ($\mathrm{kJmol^{-1}}$)

System	$E_{int}(kJmol^{-1})$	$D(10^{-9}m^2s^{-1})$
Fluorite/Water	−47.4	1.2
Calcite/Water	−69.0	0.1
Pure Water	−43.0	1.2

TABLE IV Hydration and dissolution energies of defective calcite plane ($\mathrm{kJmol^{-1}}$)

$T(K)$	E_{int}/H_2O	$E_{dis}/CaCO_3$
300	−66.9	+328.0
1000	+100.3	+135.1

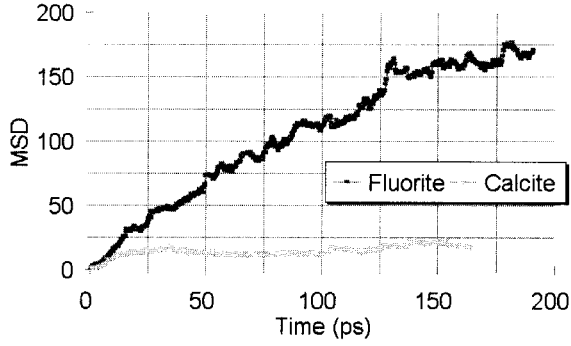

FIGURE 4 Mean square deviation of water molecules in the calcite and fluorite systems.

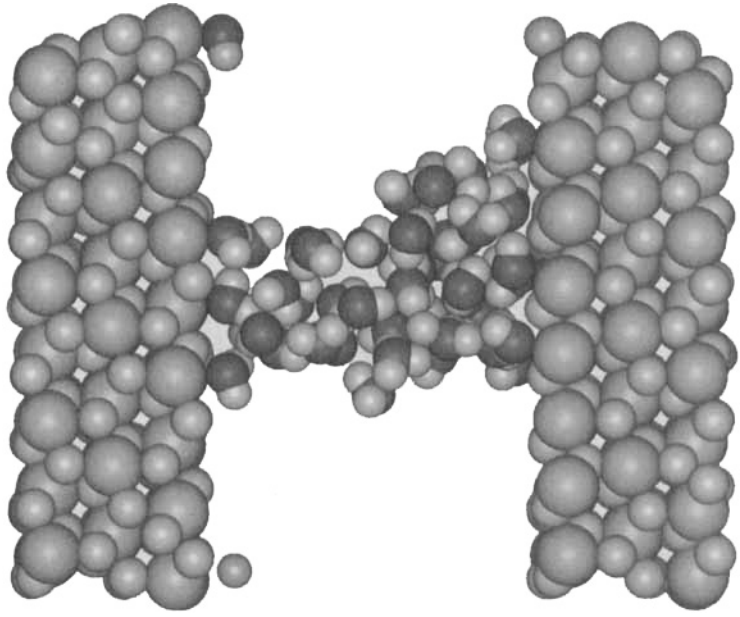

FIGURE 5 Side view of fluorite {111} planes, showing formation of a droplet of water molecules in the gap between the planes (Ca = green, F = pale blue, O = red, H = white). (See Color Plate IV).

cluster together between the surfaces. Furthermore, as a consequence of the size of our simulation cell capillary forces may also come into play, which we hope to investigate further.

At 1000 K the adsorption pattern is very similar for the two minerals. In both systems the water molecules diffuse through the gap between the

surfaces ($D = 144 \times 10^{-9}\,m^2s^{-1}$), randomly adsorbing and desorbing with large, positive interaction energies (+104.2 and +125.7 kJmol^{-1} for calcite and fluorite respectively). In order to calculate the adsorption energies at this temperature we compared the energies of the water molecules between the mineral surfaces with the self-energy of a gaseous water molecule at 1000 K.

We subsequently introduced a vacancy on the calcite $\{10\bar{1}4\}$ plane to see whether this defect would have an effect on the hydration pattern. We modelled the defective surface again at 300 K and 1000 K and calculated the average hydration energies. When a calcium carbonate unit is removed from the calcite surface the water molecules cluster in and around the defect. Figure 6a is plan view of the $\{10\bar{1}4\}$ surface with surface defect at 1000 K, clearly showing the clustering of the water molecules around the vacancy. A less pronounced clustering occurs for a defective CaF_2 surface (Fig. 6b), probably because the site of the CaF_2 vacancy is smaller than the

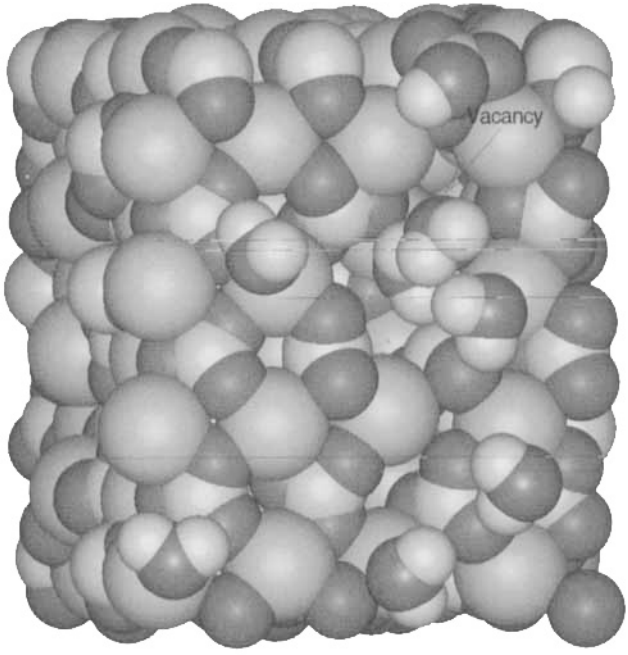

(a)

FIGURE 6 (a) Plan views of the calcite $\{10\bar{1}4\}$ surface ($T = 1000$ K) with surface $CaCO_3$ unit removed and (b) the fluorite {111} surface with surface CaF_2 unit removed, showing clustering of water molecules at the defects (Ca = green, F = pale blue, C = yellow, $O_{carbonate}$ = red, $O_{calcite\ water}$ = blue, $O_{fluorite\ water}$ = red, H = white). (See Color Plate V).

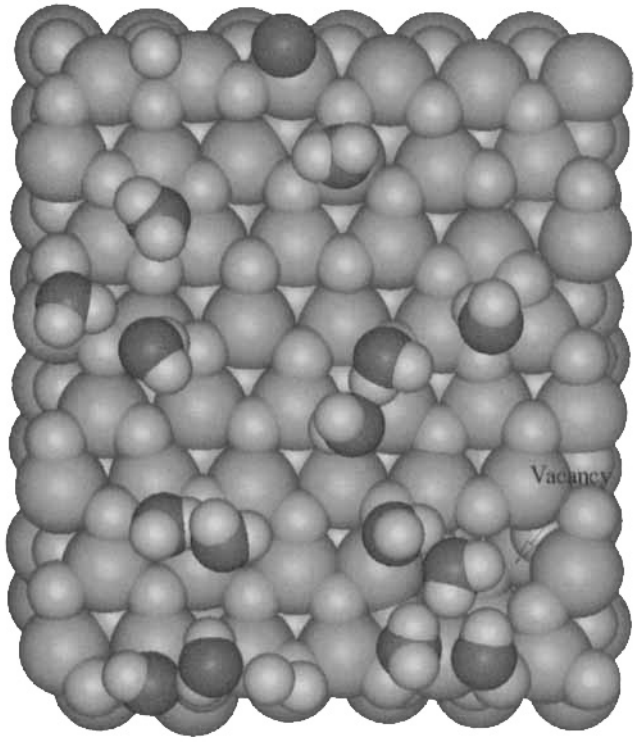

FIGURE 6 (Continued). (See Color Plate V).

site of the defect on the calcite plane, enabling a whole water molecule to adsorb in the $CaCO_3$ vacancy.

At 300 K, the interaction energy per water molecule with the defective calcite surface is calculated to be $-66.9\,kJmol^{-1}$ which increases to $+100.3$ at 1000 K (Tab. V). Comparing this to the interaction energies of the perfect surfaces at the two temperatures (-69.0 and $+104.2\,kJmol^{-1}$), we see that the interaction energies have remained the same. At 300 K any extra reactivity due to the surface defect is outweighed by the loss of the very regular adsorption pattern of the perfect surface (Fig. 1). Similarly, at 1000 K when the water molecules on the perfect surface do not adsorb in a regular pattern but diffuse through the gap adsorbing and desorbing randomly, the clustering of water molecules in and around the surface defect (Fig. 6a) is outweighed by less adsorption at other sites.

We next modelled the interaction of water with a point defect on a step on a surface, *i.e.*, interaction of the point defect with both a one-

TABLE V Surface energies and hydration energies of forsterite surfaces with water adsorbed associatively and dissociatively and associatively adsorbed water on hydroxylated surfaces

*Surface**	γ_{ass}/Jm^{-2}	γ_{dis}/Jm^{-2}	$\gamma_{ass\ on\ diss}/Jm^{-2}$	$E_{ass}/kJmol^{-1}$	$E_{ass}/kJmol^{-1}$	$E_{ass}/kJmol^{-1}$
{001}a[d]	0.47	0.52	0.08	−117.7	−120.6	−68.5
{001}b[d]	1.36	0.56	0.28	−112.9	−256.7	−64.6
{010}a	0.30	0.76	0.27	−99.4	−89.2	−71.4
{010}b[d]	0.86	0.58	0.17	−127.4	−300.1	−67.5
{100}a	1.37	2.77	–	−132.1	+73.3	–
{100}b[d]	1.28	1.34	0.78	−103.2	−168.8	−78.2
{011}a	0.28	0.33	0.16	−140.9	−172.7	−55.0
{011}b[d]	0.96	0.97	0.55	−137.0	−278.8	−72.4
{101}a[d]	1.02	0.75	0.91	−101.3	−178.5	−32.8
{101}b[d]	1.14	0.86	0.32	−117.7	−217.1	−80.1
{110}a	1.29	1.10	0.26	−171.7	−420.7	−102.3
{110}b[d]	0.35	0.49	0.20	−137.0	−150.5	−63.7
{111}a[d]	1.01	1.57	1.81	−123.5	−316.8	−126.4
{111}b[d]	0.79	0.90	0.84	−107.1	−152.4	−48.2
{021}a[d]	0.60	1.01	0.28	−130.3	−141.8	−90.7
{021}b[d]	1.50	1.28	0.32	−101.3	−167.9	−105.2

* Denotes a dipolar plane.

dimensional and a two-dimensional defect. We find at 300 K that the adsorption energy is $-67.1\,kJmol^{-1}$ which compares to $-66.9\,kJmol^{-1}$ above. Modelling these defects are important to processes such as the dissolution of calcite. The first step is to calculate the energy of removal of a $CaCO_3$ unit from the surface. In effect, we have simulated and obtained an energy for the reaction given in the following equation:

$$nCaCO_{3(s)} \longrightarrow (n-1)\,CaCO_{3(s)} + Ca^{2+}_{(aq)} + CO^{2-}_{3(aq)}$$

which we consider will be the major component of the activation energy for dissolution. The energy of dissolution of a $CaCO_3$ unit from the $\{10\bar{1}4\}$ surface is found to be $+328.0\,kJmol^{-1}$ at 300 K (Tab. V). On raising the temperature to 1000 K the dissolution energy is calculated to decrease to $+135.1\,kJmol^{-1}$ which, although much lower, even at this temperature still does not fall in the thermal energy region. Initial calculations on dissolution of calcium carbonate units from steps show that it only costs about $45.8\,kJmol^{-1}$ to remove a unit from a reactive step edge on the $\{10\bar{1}4\}$ surface. From our simulations we would therefore suggest that it is unlikely that $CaCO_3$ units dissolve from the planar cleavage plane, in agreement with experimental findings where calcite growth and dissolution was observed to occur from steps and spiral dislocations [34–36].

The interaction of adsorbing molecules with mineral surfaces is, of course, not limited to associative adsorption. Dissociative adsorption may occur, for example of water molecules leading to the adsorption of a hydrogen atom and a hydroxyl group onto the surface. In this section we

describe calculations on associative and dissociative adsorption of water onto forsterite surfaces with a view to assessing whether we can model the relative stabilities of the various surfaces correctly.

Interaction of Water with Forsterite (Mg_2SiO_4) Surfaces

Forsterite, the magnesium end member of the olivine group of minerals, consists of SiO_4 tetrahedra linked by magnesium cations in octahedral coordination. This prominent Mantle material has an orthorhombic structure with spacegroup Pbnm. We modelled both dissociative and associative adsorption of water on the low-index surfaces. Dissociative adsorption lead to hydroxylated surfaces with terminal -MgOH and -SiOH groups. Table V shows the surface energies and hydration energies of the planes with both associatively and dissociatively adsorbed water molecules. In addition we adsorbed water molecules onto the hydroxylated surfaces. The energies given in Table V indicate that some surfaces, *e.g.*, the non-dipolar {101} and {100} planes, are predicted not to be hydroxylated and the water molecules will remain associatively adsorbed, whereas the other surfaces, especially the non-dipolar {110} and the dipolar {010} and {111} a planes, prefer dissociative adsorption.

At present there are no experimental results to test our predictions. However, we can get a guide to the changing surface stability by modelling the equilibrium morphologies. The equilibrium morphology of a crystal is obtained from the surface energies, by assuming a crystal adopts a shape to lower its surface energy and hence provides a measure of the relative stabilities of the surfaces. Figure 7(a) shows a common experimental

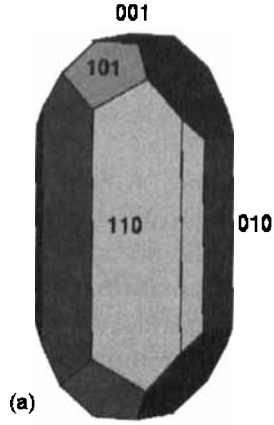

FIGURE 7 (a) Experimental and (b) calculated morphology of forsterite.

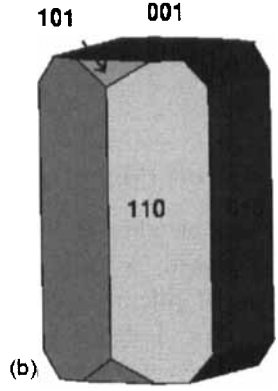

FIGURE 7 (Continued).

morphology expressing surfaces investigated in this paper [37]. From the collection of surface energies of the hydrated and hydroxylated surfaces we calculated an equilibrium morphology for forsterite (Fig. 7b). There is a good comparison between the morphology thus obtained with the experimental morphology: the same surfaces are expressed in the calculated equilibrium morphology as are found in the experimental morphology, although both {001} and {110} surfaces are somewhat too stable with respect to the {101} and {021} planes.

CONCLUSION

This study has shown that atomistic simulation techniques are well placed to provide an insight at the atomic level into the interactions between substrate and adsorbate molecules. Our calculations on the competitive adsorption of water and methanoic acid at calcite and fluorite surfaces provide an explanation for experimental findings in mineral processing techniques.

Molecular dynamics simulations of the hydration of the planar calcite $\{10\bar{1}4\}$ and fluorite {111} surfaces shows a very different adsorption pattern at both surfaces. On the calcite surface water adsorbs in a very regular pattern with a network of hydrogen-bonding intermolecularly between the water molecules and to the surface atoms. On fluorite the water molecules prefer to cluster together and form a droplet between the surfaces rather than wet the surface homogeneously. At high temperature both the regular adsorption pattern at the calcite surface and the formation of a

droplet on the fluorite surface is disturbed with the water molecules moving freely through the gap.

On introduction of a surface defect the regular adsorption pattern at the calcite surface is disturbed leading to a decrease in the adsorption energy. However, at high temperature the surface defect induces clustering of the water molecules at the vacancy making the average hydration energy less endothermic. Dissolution from the calcite surface is shown to be energetically very costly at both temperatures, but not as endothermic when calcium carbonate units are removed from steps.

The calculated equilibrium morphology of forsterite obtained using the surface energies of the various hydrated surfaces agrees well with the experimentally found morphology indicating that the relative stabilities of the surfaces were modelled correctly.

Acknowledgement

We thank EPSRC grant no. GR/L35577 and NERC grant no. GR3/11779 for financial support and Molecular Simulations Inc. for InsightII.

References

[1] de Leeuw, N. H., Watson, G. W. and Parker, S. C. (1996). "Atomistic simulation of adsorption of water on three-, four- and five-coordinated surface sites of magnesium oxide", *J. Chem. Soc. Faraday Trans.*, **92**, 2081.

[2] de Leeuw, N. H., Higgins, F. M. and Parker, S. C. (1998). "Modelling the surface structure and stability of a-quartz", *J. Phys. Chem. B*, **103**, 1270.

[3] de Leeuw, N. H. and Parker, S. C. (1998). "Molecular-dynamics simulation of MgO surfaces in liquid water using a shell-model potential for water", *Phys. Rev. B*, **58**, 13901.

[4] de Leeuw, N. H. and Parker, S. C. (1998). "Surface structure and stability of the calcium carbonate polymorphs calcite, aragonite and vaterite: an atomistic approach", *J. Phys. Chem. B*, **102**, 2914.

[5] de Leeuw, N. H. and Parker, S. C. (1999). "The effect of chemi- and physisorption of water on the surface structure and stability of alpha-Alumina", *J. Am. Ceram. Soc.*, accepted.

[6] Oliver, P. M., Watson, G. W., Kelsey, E. T. and Parker, S. C. (1997). "Atomistic simulation of the surface structure of the TiO_2 polymorphs rutile and anatase", *J. Mater. Chem.*, **7**, 563.

[7] Mackrodt, W. C., Davey, R. J., Black, S. N. and Docherty, R. (1987). "The morphology of a-Al_2O_3 and a-Fe_2O_3: the importance of surface relaxation", *J. Cryst. Growth*, **80**, 441.

[8] Oliver, P. M., Parker, S. C., Egdell, R. G. and Jones, F. H. (1996). "Computer simulation of the surface structures of WO_3", *J. Chem. Soc. Faraday Trans.*, **92**, 2049.

[9] de Leeuw, N. H., Watson, G. W. and Parker, S. C. (1995). "Atomistic simulation of the effect of dissociative adsorption of water on the surface structure and stability of calcium and magnesium oxide", *J. Phys. Chem.*, **99**, 17219.

[10] de Leeuw, N. H., Redfern, S. E. and Parker, S. C. (1998). "Atomistic simulation of the effect of molecular adsorption of water on the structure and stability of mineral surfaces", *Recent Res. Devel. Phys. Chem.*, **2**, 441.

[11] Tasker, P. W. (1979). "The surface energies, surface tensions and surface structure of the alkali halide crystals", *Phil. Mag. A*, **39**, 119.
[12] Tasker, P. W. (1979). "The stability of ionic crystal surfaces", *J. Phys. C: Solid State Phys.*, **12**, 4977.
[13] Mackrodt, W. C. and Stewart, R. F. (1979). "Defect properties of ionic solids: II. Point defect energies based on modified electron-gas potentials", *J. Phys. C: Solid State Phys.*, **12**, 431.
[14] Bertaut, F. (1958). *Compt. Rendu.*, **246**, 3447.
[15] Benson, G. L. and Yon, K. S., *The Solid Gas Interface*, Flood, E. A. Ed. Arnold, London, 1967.
[16] Pavese, A., Catti, M., Parker, S. C. and Wall, A. (1996). "Modelling of the thermal dependence of structural and elastic properties of calcite $CaCO_3$", *Phys. Chem. Minerals*, **23**, 89.
[17] Catlow, C. R. A., Norgett, M. J. and Ross, A. (1977). *J. Phys. C*, **10**, 1630.
[18] Lewis, G. V. and Catlow, C. R. A. (1985). "Potential models for ionic oxides", *J. Phys. C: Solid State Phys.*, **18**, 1149.
[19] Sanders, M. J., Leslie, M. and Catlow, C. R. A. (1984). "Interatomic potentials for SiO_2", *J. Chem. Soc. Chem. Commun.*, p. 1271.
[20] Price, G. D., Parker, S. C. and Leslie, M. (1987). "The lattice dynamics of forsterite", *Mineral. Mag.*, **51**, 157.
[21] Parker, S. C. and Price, G. D. (1989). "Computer modelling of phase transitions in minerals", *Adv. Solid State Chem.*, **1**, 295.
[22] Osguthorpe, P., Osguthorpe, D. and Hagler, A. (1988). *Proteins; Structure, Function and Genetics*, **14**, 31.
[23] Liang, Y., Baer, D. R., McCoy, J. M., Amonette, J. E. and LaFemina, J. P. (1996). "Dissolution kinetics at the calcite-water interface", *Geochim. Cosmochim. Acta*, **60**, 4883.
[24] Beruto, D. and Giordani, M. (1993). "Calcite and aragonite formation from aqueous calcium hydrogencarbonate solutions: effect of induced electromagnetic field on the activity of $CaCO_3$ nuclei precursors", *J. Chem. Soc. Faraday Trans.*, **89**, 2457.
[25] Goni, S., Sobrados, L. and Hernandez, M. S. (1993). "Increase of acid-surface reactivity through water molecules adsorption process: V_2O_5-$CaCO_3$ behaviour", *Solid State Ionics*, **63**, 786.
[26] Ohnesorge, F. and Binnig, G. (1993). "True atomic resolution by atomic force microscopy through repulsive and attractive forces", *Science*, **260**, 1451.
[27] Heywood, B. R. and Mann, S. (1994). "Molecular construction of oriented inorganic materials: controlled nucleation of calcite and aragonite under compressed Langmuir monolayers", *Chem. Mater.*, **6**, 311.
[28] de Leeuw, N. H. and Parker, S. C. (1997). "Atomistic simulation of the effect of molecular adsorption of water on the surface structure and energies of calcite surfaces", *J. Chem. Soc. Faraday Trans.*, **93**, 467.
[29] Gilman, J. J. (1960). "Direct measurements of the surface energies of crystals", *J. Appl. Phys.*, **31**, 2208.
[30] Liang, Y., Lea, A. S., Baer, D. R. and Engelhard, M. H. (1996). "Structure of the cleaved $CaCO_3$ surface in an aqueous environment", *Surf. Sci.*, **351**, 172.
[31] Mielczarski, J. A., Mielczarski, E. and Cases, M. (1999). "Dynamics of fluorite-oleate interactions", *Langmuir*, **15**, 500.
[32] Forester, T. R. and Smith, W. (1995). *DL_POLY user manual*, (CCLRC, Daresbury Laboratory, Daresbury, Warrington, UK).
[33] Duan, Z., Moller, N. and Weare, J. H. (1995). "Molecular dynamics simulation of water properties using RWK2 potential: from clusters to bulk water", *Geochim. Cosmochim. Acta*, **59**, 3273.
[34] Gratz, A. J., Hillner, P. E. and Hansma, P. K. (1993). "Step dynamics and spiral growth on calcite", *Geochim. Cosmochim. Acta*, **57**, 491.
[35] Hillner, P. E., Manne, S. and Hansma, P. K. (1993). "Atomic force microscope: a new tool for imaging crystal growth processes", *Faraday Discuss.*, **95**, 191.
[36] MacInnes, I. N. and Brantley, S. L. (1992). "The role of dislocations and surface morphology in calcite dissolution", *Geochim. Cosmochim. Acta*, **56**, 1113.
[37] Deer, W. A., Howie, R. A. and Zussman, J., *An introduction to the rock-forming minerals*, Longman Group, Harlow, 1992.